CYTOCHEMICAL AND DEVELOPMENTAL CHANGES IN MICROBODIES (GLYOXYSOMES) AND RELATED ORGANELLES OF CASTOR BEAN ENDOSPERM

EUGENE L. VIGIL

From the Whitman Laboratory, The University of Chicago, Chicago, Illinois 60637

ABSTRACT

Structural changes in endosperm cells of germinating castor beans were examined and complemented with a cytochemical analysis of staining with diaminobenzidine (DAB). Deposition of oxidized DAB occurred only in microbodies due to the presence of catalase, and in cell walls associated with peroxidase activity. Seedling development paralleled the disappearance of spherosomes (lipid bodies) and matrix of aleurone grains in endosperm cells. 6 to 7 days after germination, a cross-section through the endosperm contained cells in all stages of development and senescence beginning at the seed coat and progressing inward to the cotyledons. Part of this aging process involved vacuole formation by fusion of aleurone grain membranes. This coincided with an increase in microbodies (glyoxsomes), mitochondria, plastids with an elaborate tubular network, and the formation of a new protein body referred to as a dilated cisterna, which is structurally and biochemically distinct from microbodies although both apparently develop from rough endoplasmic reticulum (ER). In vacuolate cells microbodies are the most numerous organelle and are intimately associated with spherosomes and dilated cisternae. This phenomenon is discussed in relation to the biochemical activities of these organelles. Turnover of microbodies involves sequestration into autophagic vacuoles as intact organelles which still retain catalase activity. Crystalloids present in microbodies develop by condensation of matrix protein and are the principal site of catalase formerly in the matrix.

INTRODUCTION

Although microbodies have only recently been established as ubiquitous organelles of plant cells (26, 47), their importance in cellular metabolism clearly emerged from recent studies on endosperm and leaf tissue (19). The demonstration of several glyoxylate cycle enzymes in a particulate fraction from castor bean endosperm (12) focused attention on a new compartmentalized enzyme system in plant cells. Examination of purified particles by electron microscopy (13) showed them to be single-membrane-bounded organelles with a gran-ular matrix. Besides containing the two essential enzymes of the glyoxylate cycle, isocitrate lyase and malate synthetase, these organelles also contained glycolate oxidase, aconitase, and catalase and were, therefore, termed glyoxysomes by Breidenbach et al. (13). Further study of the enzyme complement in this organelle by Cooper and Beevers (15, 16) has shown that all enzymes required for both β-oxidation and the glyoxylate cycle are present in the glyoxysome with a very active catalase which oxidizes endogenously

formed hydrogen peroxide. Thus the enzymes involved in succinate formation from acyl-CoA units are confined to a single organelle.

Since the glyoxysome is the only site of catalase in castor bean endosperm, this organelle can be positively identified at the ultrastructural level by using a cytochemical procedure for catalase (64). The reaction is based on the oxidation of a suitable proton donor, in this case 3,3'-diaminobenzidine (DAB), by the peroxidatic action of catalase, first demonstrated for beef liver catalase by Keilin and Hartree (37). Oxidation occurs in the presence of a low concentration of hydrogen peroxide and follows Novikoff and Goldfisher's modification (48) of Graham and Karnovsky's original DAB procedure for peroxidase (33). Peroxidatic activity of catalase in microbody staining in liver cells of the rat has recently been demonstrated by Fahimi (23).

Germinating castor bean seeds provide an opportunity to investigate the rapid development of glyoxysomes in endosperm cells as stored food reserves are depleted and cellular breakdown (senescence) occurs. The structure, development, and identity of glyoxysomes, as well as their interrelationships with other cellular organelles, may, therefore, be firmly established. The present analysis of ultrastructural and cytochemical changes in endosperm cells during seed germination establishes equivalence between microbodies and glyoxysomes, the constitutent nature of microbodies in endosperm cells, and documents their origin and fate.

MATERIALS AND METHODS

Tissue Preparation

Seeds of castor bean, *Ricinus communis* L., variety "Zanzibariensis," were imbibed for 14–16 hr in aerated tap water at room temperature, placed in moistened vermiculite, and grown under greenhouse conditions. Endosperm tissue, circa 1 mm², collected at various intervals from imbibition until the texture and color of the tissue had become soft and yellow were fixed in glutaraldehyde followed by osmium tetroxide.

Cytochemical Procedure

Rinsed glutaraldehyde-fixed tissue was either cut into small sections under a binocular microscope or sectioned at 40 μ on an Oxford Vibratome (Oxford Laboratories, San Mateo, Calif.) before incubation in DAB media for 60 min at 37°C. The complete re-

action medium freshly prepared for each experiment contained the following: 5.0 ml 0.05 M 2-amino-2-methyl-1,3-propandiol buffer (AMP); 0.1 ml 3% hydrogen peroxide diluted fresh from 30% Superoxol (Merck & Co., Inc., Rahway, N. J.); 10.0 mg 3,3'-diaminobenzidine tetrahydrochloride (DAB) (Sigma Chemical Co., St. Louis, Mo.). The final pH was adjusted to 9.0 before tissue sections were added.

For all experiments tissue sections were equilibrated in 0.1 M AMP, pH 9.0, prior to incubation in the reaction media. The same buffer was used as a rinse solution after incubation and was followed by several rinses in 0.1 M cacodylate buffer, pH 7.4. Osmication, dehydration, and embedding in plastic followed the procedure described below.

In order to determine whether catalase alone was responsible for oxidation of DAB, the complete reaction medium was varied by the addition of different inhibitors or by removal of hydrogen peroxide along with the addition of inhibitors. For all inhibitor studies the tissue sections were incubated for at least 1 hr (37°C) in media containing the inhibitors but not DAB, thus insuring sufficient penetration of the inhibitor and interaction with the enzyme(s) under investigation.

Electron Microscopy

Tissue sections were prefixed in 2.5% glutaraldehyde (Polysciences, Inc. Rydel, Pa.) in 0.05 M cacodylate buffer, pH 7.4. Following a 6 hr glutaraldehyde fixation at 4°C, tissue sections were washed in the cold for 40 hr in the same buffer (0.1 M) and either used for cytochemistry or postosmicated. After osmication in 2% osmium tetroxide in 0.05 M cacodylate buffer, pH 7.4, for 2 hr at 4°C, tissue sections were dehydrated at room temperature in an acetone series followed by propylene oxide and embedded in Araldite-Epon. To enhance the contrast of cellular structures during dehydration, fixed tissue sections from several samples were left overnight in 70% acetone containing 2% uranyl acetate. Thin sections of plastic-embedded tissue were stained in either aqueous 2% uranyl acetate followed by lead citrate (53), or just lead citrate for material previously treated with uranyl acetate during dehydration. Thin sections were viewed in either a Hitachi HU 11-A electron microscope at 75 kv or a Siemens Elmiskop 1 at 80 kv.

Light Microscopy

For light microscopy, 1 μ sections of Araldite-Epon embedded tissue were lightly stained with warm 1% toluidine blue in 2% sodium borate before examination with phase optics. The phase-contrast image of these sections was recorded on Kodak M plates (4" × 5") with use of a green filter.

RESULTS

Tissue Structure

6–7 days after germination, all the changes in fine structure in the endosperm observed throughout the study could be seen along a cross-section extending from the seed coat inward to the cotyledons in the center of the seed. The earliest changes in cellular structure occurred in cells close to the cotyledons and progressed continuously to the cells neighboring the seed coat. Thus in such a cross-section, which we have divided into four zones, endosperm cells nearest the cotyledons have progressed furthest while those near the seed coat show changes in fine structure that are just being initiated and they resemble cells from imbibed tissue. The frequencies of various organelles in Zones II and III are given in Table I.

ZONE I: The endosperm cells nearest the seed coat contain an abundance of tightly packed lipid bodies or spherosomes (Fig. 1). Interspersed among the spherosomes are large aleurone grains (Figs. 1 and 9). These organelles range in size from 2 to 9 μ, and have a single enclosing membrane and a densely staining fibrous matrix which contains large compact crystalloids and smaller phytin-containing globoids (62) (Figs. 1 and 9). In addition to these two prominent organelles, three other structures resembling proplastids, promitochondria, and microbodies can also be seen in Fig. 1.

The proplastids usually lack lamellae and starch grains and have a granular matrix with only a few osmiophilic granules embedded in it (arrows, Fig. 1). Promitochondria possess even fewer characteristic structures and only appear as distorted double-membrane-bounded organelles which have no recognizable cristae (inset, Fig. 1). Microbodies, being the smallest organelle, are few in number and have a granular matrix of less density than aleurone grains but do not have nucleoids characteristic of microbodies in other zones.

ZONE II: Endosperm cells in this zone have fewer spherosomes than those in Zone I, yet mitochondria, plastids, and microbodies are more numerous as illustrated in Fig. 2. Free ribosomes, rough endoplasmic reticulum (ER), and dictyosomes, evident for the first time, are interspersed among these organelles (Fig. 2). Aleurone grains appear swollen and, accompanying this swollen condition, there is evidence of disaggregation of the crystalloid structure (Fig. 10). The aleurone grain matrix is either dispersed (Fig. 10) or aggregated along the limiting membrane (Fig. 2). As these organelles swell, they become appressed, their membranes fuse, eventually breakdown, and finally a larger more vacuolate structure is formed that displaces the cytoplasm to the periphery of the cell.

In contrast to Zone I, plastids in Zone II have several well-developed lamellae or tubules (Fig. 3), DNA-like strands, and an occasional starch grain (Fig. 2). Crista development in mitochondria, on the other hand, has just begun in Zone II cells, most of the matrix region containing only fibrous material, DNA-like strands, and small granules, possibly ribosomes (Fig. 4).

Microbodies are more numerous in these cells but still do not contain any nucleoids (Fig. 2). In Zone I the microbodies have a fairly uniform diameter of about 0.8 μ, whereas here they range in size from 0.2 to 0.8 μ. The common occurrence of rough ER in these cells may account for the numerous, small microbodies.

ZONE III: Characteristic of this zone are cells with large vacuoles that restrict most of the cytoplasm to regions along the cell wall (Figs. 5 and 12). These vacuoles form from limiting membranes of aleurone grains. Spherosomes, prominent in Zone I, are not very conspicuous (Figs. 5 and 12) and when present in a section are surrounded by microbodies (inset, Fig. 5).

Development of internal structures in plastids and mitochondria is much more extensive (Figs. 5 and 16). Invaginations of the inner plastid envelope (Fig. 7) result in the formation of a network of interconnected tubules, approximately 400 A in diameter, which has an over-all netlike appearance when fully developed (Fig. 16). Mitochondria now have many well-developed cristae which fill most of the organelle (Figs. 5 and 16).

Two single membrane-bounded organelles present in these cells can be distinguished by both structure and contents, typical microbodies and dilated cisternae (Figs. 5 and 7). Microbodies, being more numerous, are easily distinguished from other protein bodies by the lack of surface-bound ribosomes and the presence of characteristic nucleoids (Figs. 7 and 8). While microbodies vary in shape from spherical to ellipsoidal with a range in diameter from 0.2 to 1.7 μ, dilated cisternae are spherical (Figs. 5, 7, 8, and 16) with a diameter averaging 0.9 μ. Moreover, the matrix in microbodies is dispersed throughout the interior and is not separated from the limiting membrane by a clear mantle as is true of dilated cisternae (Fig. 8).
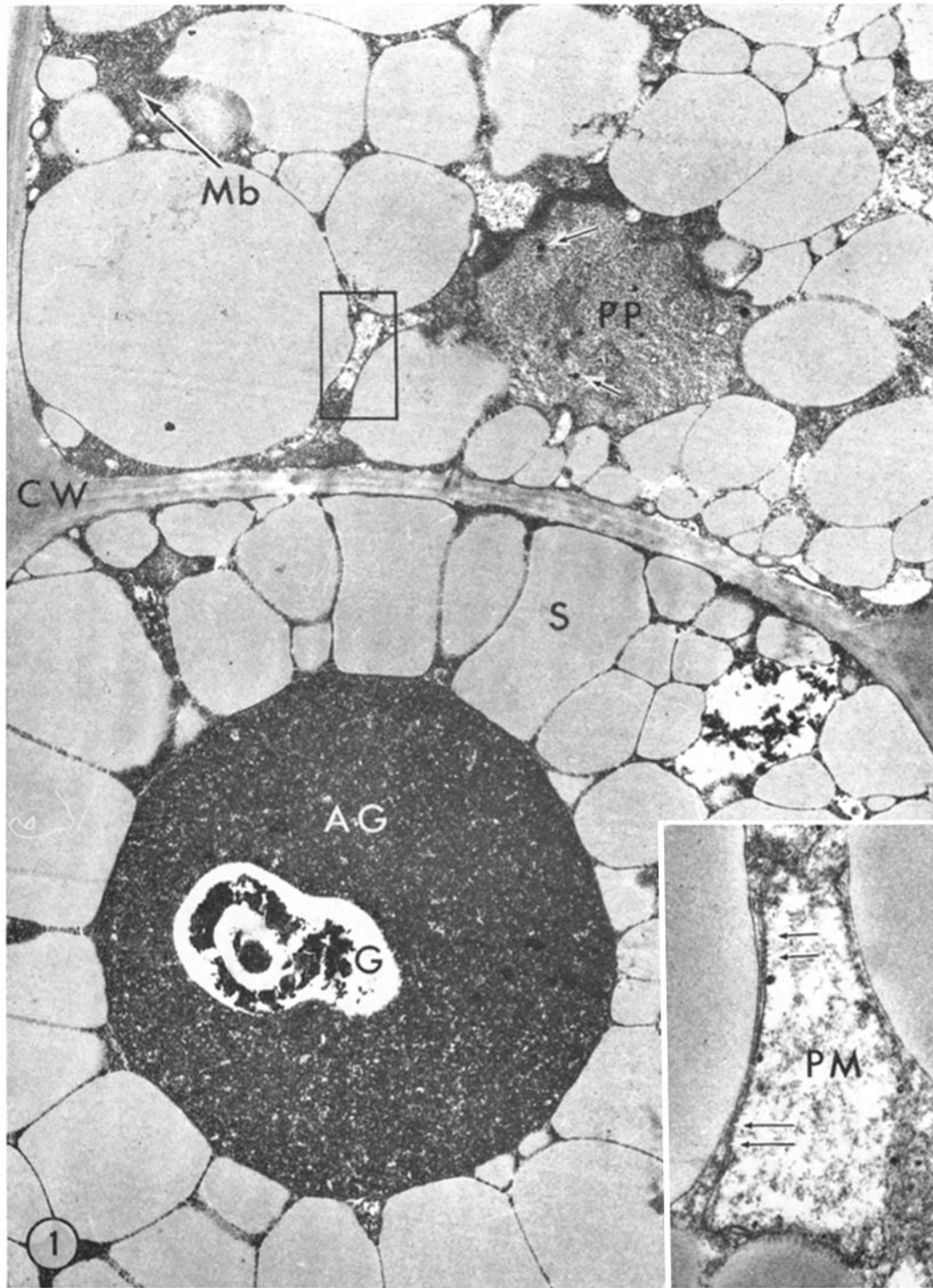
FIGURE 1 Portion of two adjacent endosperm cells following inhibition (Zone I). Spherosomes (S) are tightly packed, with aleurone grains (AG), proplastids (PP), microbodies (Mb), and double-membrane-bounded organelles (blocked off region) being the only other recognizable organelles. Cell wall (CW); osmiophilic granules (arrows); globoid (G). Tissue stained with uranyl acetate during dehydration. Section contrasted with lead citrate. × 12,000. Inset shows one of the double-membrane-bounded organelles in greater detail. Absence of protruding cristae along inner membrane (arrows) suggests that this is probably a promitochondrion (PM). Same staining. × 24,000.
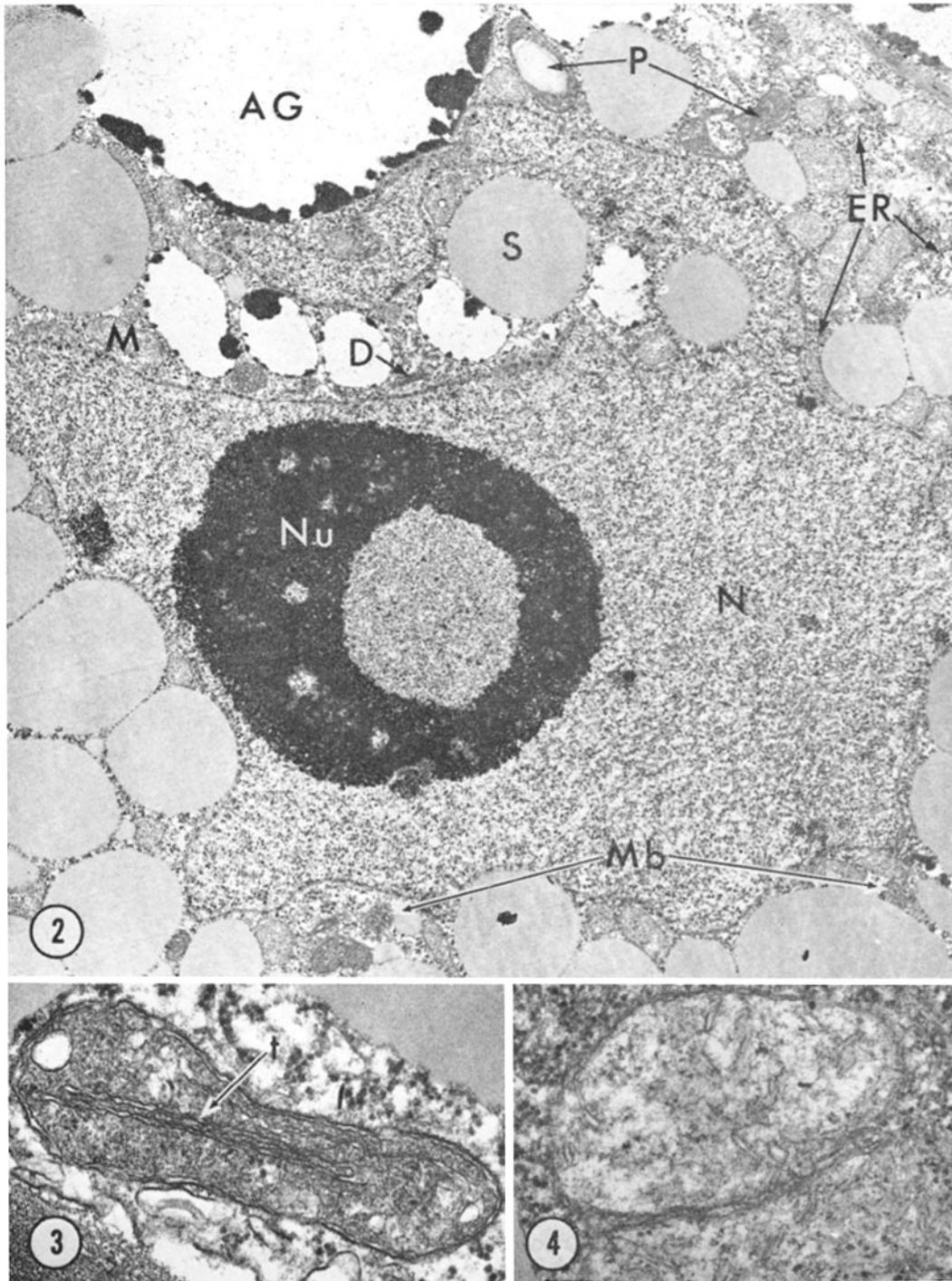
FIGURE 2   Section of an endosperm cell from Zone II. Spherosomes (S) are fewer in number, providing more room for other cytoplasmic structures around the nucleus (N). Mitochondria (M) and plastids (P) are more evident whereas aleurone grains (AG) appear vacuolate. Several microbodies (Mb) are present, as are rough endoplasmic reticulum (ER), free ribosomes, and dictyosomes (D). Nucleolus (Nu). Uranyl acetate/lead citrate (UA/Pb). × 9100.

FIGURE 3   Enlargement of a plastid, illustrating several characteristic tubules or lamellae (t). UA/Pb. × 40,000.

FIGURE 4   Two mitochondria at a higher magnification to show the sparse and dispersed cristae therein. UA/Pb. × 41,600.

The similarity between these ribosome-bearing organelles and dilated cisternae of ER in radish root cells (11) suggests that they may arise from rough ER. A direct connection with rough ER is shown in Fig. 8. Of particular interest is the continuity between the fibrous contents of the connecting portion of ER and the matrix of the organelle proper. A section tangential to the membrane surface reveals the presence of ribosomes in polysome configurations (*inset*, Fig. 8).

ZONE IV: The cells in Zone IV, adjacent to the cotyledons, have lost their cytoplasmic contents. The final stages of cellular breakdown are abrupt and very sudden, resulting in complete disruption of both cytoplasm and cell walls which produces a line of demarcation between living and nonliving cells. This region is only 2–5 cell layers thick, with most cells in final stages of cellular dissolution.

Microbodies

DISTRIBUTION AND DEVELOPMENT: While microbodies are present in all zones except Zone IV, and, therefore, a constituent organelle of castor bean endosperm, they become most abundant and possess their characteristic inclusions in Zone III. Also in Zone III the plastids, mitochondria, and dilated cisternae become most fully differentiated. Table I shows the distribution of these organelles per 100 μ^2 in cells of Zones II and III. There is approximately a fivefold increase in microbodies per unit area. Moreover, in Zone III cells microbodies are almost twice as numerous as

TABLE I

Organelle Profiles (per 100 μ^2)* in Cells of Zones II and III

| Organelle	Mean and standard error	
	Zone II	Zone III
Microbodies	9.5 ± 1.6	44.6 ± 6.4
Mitochondria	14.8 ± 2.5	25.0 ± 7.0
Plastids	1.3 ± 0.5	4.4 ± 0.9
Dilated cisternae	0	7.7 ± 1.9

* Approximations were made to exclude aleurone grains, nucleus, and vacuoles from total area scored.

mitochondria, in comparison to their almost equal number in Zone II. Spherosomes, on the other hand, are reduced in number in Zone III cells, doubtless reflecting their utilization in conjunction with the surrounding microbodies. Mitochondria show an approximate twofold increase, in comparison to the threefold increase in plastids between Zones II and III. It is only in Zone III cells that dilated cisternae appear, and they account for 9% of organelles scored. The attachment of rough ER to microbodies and dilated cisternae (Figs. 6–8) suggests a direct mode of origin from ER. Fibrous material in the ER cisternae (Figs. 6 and 8) closely resembles that in the matrix of the organelles and may represent newly synthesized protein from the surface-bound polysomes.

INCLUSIONS: The presence of crystalline and amorphous inclusions in a small number of microbodies in Zone III cells may indicate organelle

FIGURE 5 Section of a vacuolate endosperm cell in Zone III. Although aleurone grains are absent from the cytoplasm, a few spherosomes (*S*) still remain. Other cytoplasmic structures include ameboid plastids (*P*), well-developed mitochondria (*M*), a new protein body (*DC*), and numerous microbodies (*Mb*) several of which are closely associated with spherosomes. Not all microbodies are free in the cytoplasm, as indicated by the presence of a microbody in a small, double-membraned vacuole (arrow). Dictyosomes (*D*) are also present. UA/Pb. × 7400. The intimate association between microbodies and spherosomes is shown in greater detail in the *inset* where eight microbodies are apposed to a single spherosome. UA/Pb. × 15,700.

FIGURE 6 Three microbodies with attached segments of rough *ER*. The connecting region is not always terminal (arrow). A polysome (*Ps*) configuration is present on the surface of an ER segment continuous with the microbody membrane. UA/Pb. × 83,000. In the *inset*, the connecting segment of ER contains granular to fibrillar material of a density similar to that in the microbody matrix. The asterisk lies over a denser central region of the microbody matrix which appears to be paracrystalline. UA/Pb. × 41,500.
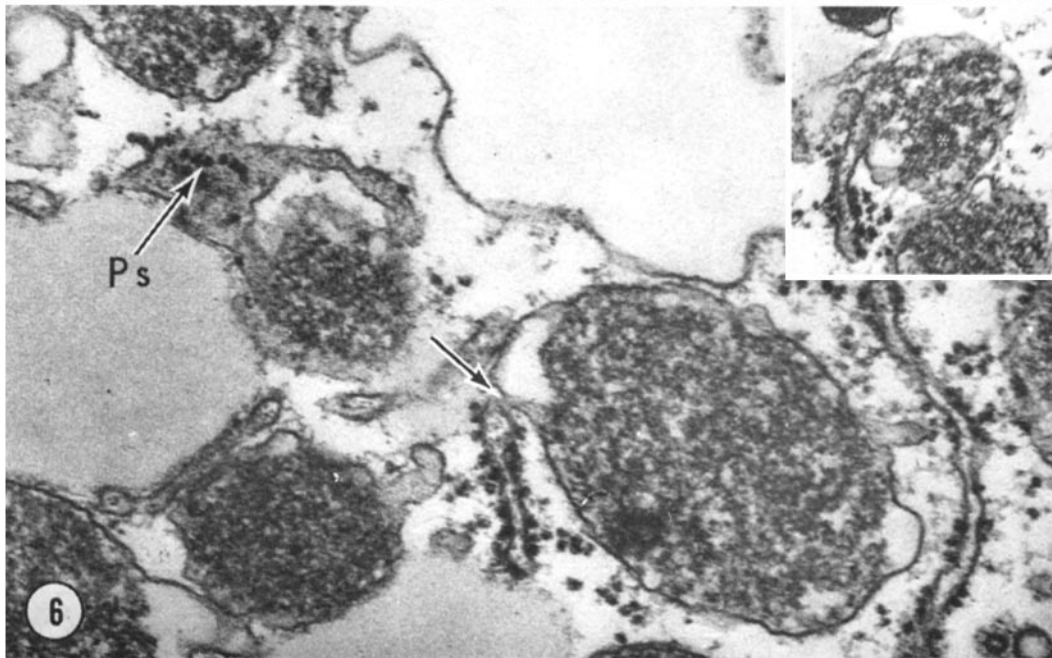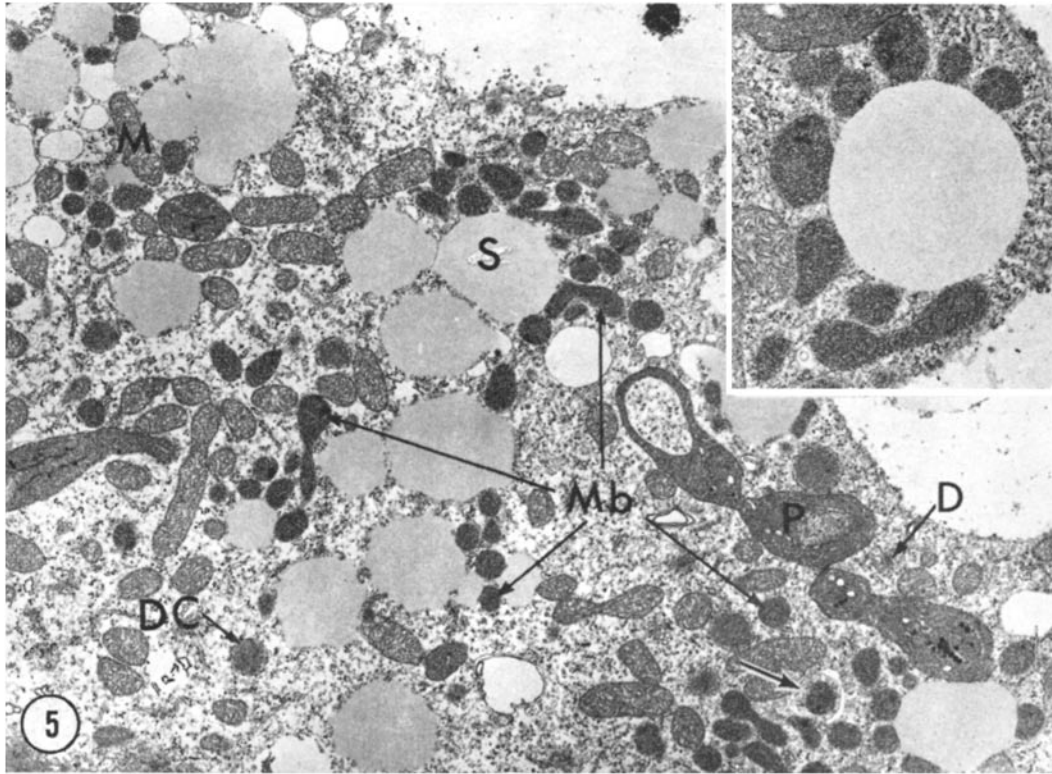
"differentiation" as found in differentiating root and coleptile cells (manuscript in preparation). The inclusions differ in structure and distribution within the organelle. The very electron-opaque, amorphous inclusion is most frequently situated at or along the enclosing membrane, whereas the crystalloid is centrally located (Fig. 7). The basic units of the crystalloid are dense rods, 60 A in diameter, arranged in a cross-band pattern with a lattice spacing of 110 A. Crystalloid enlargement apparently occurs along the edges confluent with the matrix by addition of fibrous material. Analysis of serial sections cut through the crystalloid indicates that this structure is a rectangular prism, displaying in cross-section a series of interconnected rectangular or tetrangular units (Fig. 18). Oblique sections through this prism show different patterns ranging from diamonds (*inset*, Fig. 7) to a series of parallel lines.

INTERASSOCIATION WITH OTHER ORGANELLES: The appressed and distorted appearance of organelles in Zone I cells changes with the disappearance of spherosomes and their replacement by areas of ground cytoplasm. The intimate association between microbodies and spherosomes and dilated cisternae is, however, still maintained in Zone III. Similar interactions between microbodies and other organelles are also apparent in leaf cells (24). The close spatial apposition of microbodies and spherosomes and, to a lesser extent, dilated cisternae is shown in Figs. 5 and 16, where contact between organelles is often so close that separate limiting membranes are no longer apparent. Where dilated cisternae and microbodies are closely appressed, ribosomes are absent from

the apposed portion of the dilated cisternal membrane (*inset*, Fig. 16).

TURNOVER: Microbodies apparently are removed from the cytoplasm as intact organelles by a process of autophagic vacuole formation (Figs. 5, 14, and 15). Sequestration of small areas of cytoplasm involves the enveloping action of smooth cisternae (Fig. 14), forming a double membrane-bounded vacuole. These membranes gradually fuse (arrows, Fig. 14) into a single membrane approximately 150 A in thickness. Autophagic vacuoles are common to cells of Zone III and appear only to contain microbodies, a few segments of rough ER, and free ribosomes. Their formation appears to be strikingly similar to the sequestration process in animal cells (60). To our knowledge, the process has not been described in plants.

Dilated cisternae in cells bordering on Zone IV are not sequestered from the cytoplasm but shrink as their matrix material disappears. These vesiculate structures decrease in size to roughly half their original diameter, 0.4 μ vs. 0.9 μ, and eventually resemble profiles of slightly swollen rough endoplasmic reticulum.

Cytochemical Localization of Catalase and Peroxidase

Peroxidatic activity of peroxidase and/or catalase is indicated by browning of the tissue after incubation of glutaraldehyde-fixed endosperm sections in an alkaline medium for 60 min at 37°C. Postosmication converts the oxidized DAB to osmium black (54). Light microscopic examination of these sections shows a particulate distribution of

---

FIGURE 7 Four microbodies (*Mb*) in a Zone II cell, with three containing either crystalline and/or amorphous inclusions. A smooth or rough-surfaced tail is visible on two microbodies (arrows). The structural features of a dilated cisterna (DC) stand out in striking contrast to the neighboring microbodies. Invaginations of the inner membrane of the plastid (white arrows) are continuous with the tubules (*t*), indicating the mode of formation. UA/Pb. $\times$ 29,500. The crystalloid in the microbody shown in the *inset* has a diamond pattern often observed in these organelles. Tissue stained with uranyl acetate. Section contrasted with lead citrate. $\times$ 50,000.

FIGURE 8 Detail view of the connecting region between rough *ER* and a dilated cisterna (*DC*). The clear continuity between the matrix and fibrous material in the *ER* not only accentuates the connection but also indicates a possible source of matrix. The delicate connection of *ER* to a microbody (*Mb*) shown by the arrow is not very clear and appears constricted. Tissue stained with uranyl acetate. Section contrasted with lead citrate. $\times$ 43,300. The *inset* is a tangential section of a dilated cisterna illustrating the polysome arrangement of surface-bound ribosomes. Same staining. $\times$ 60,000.
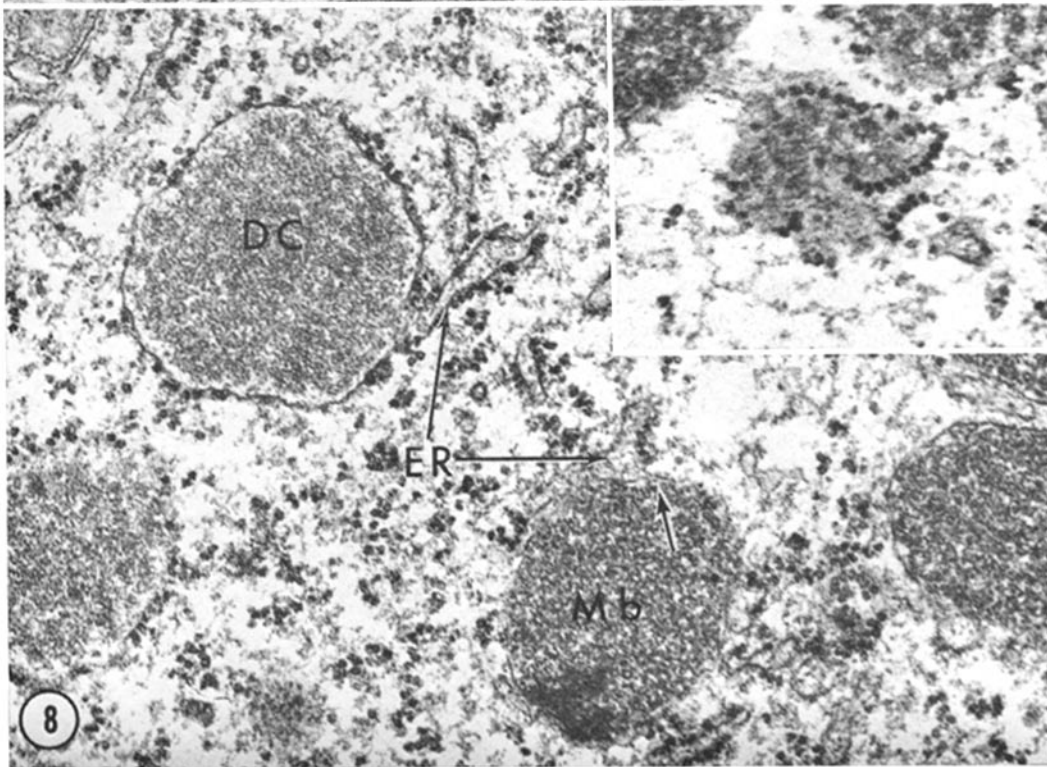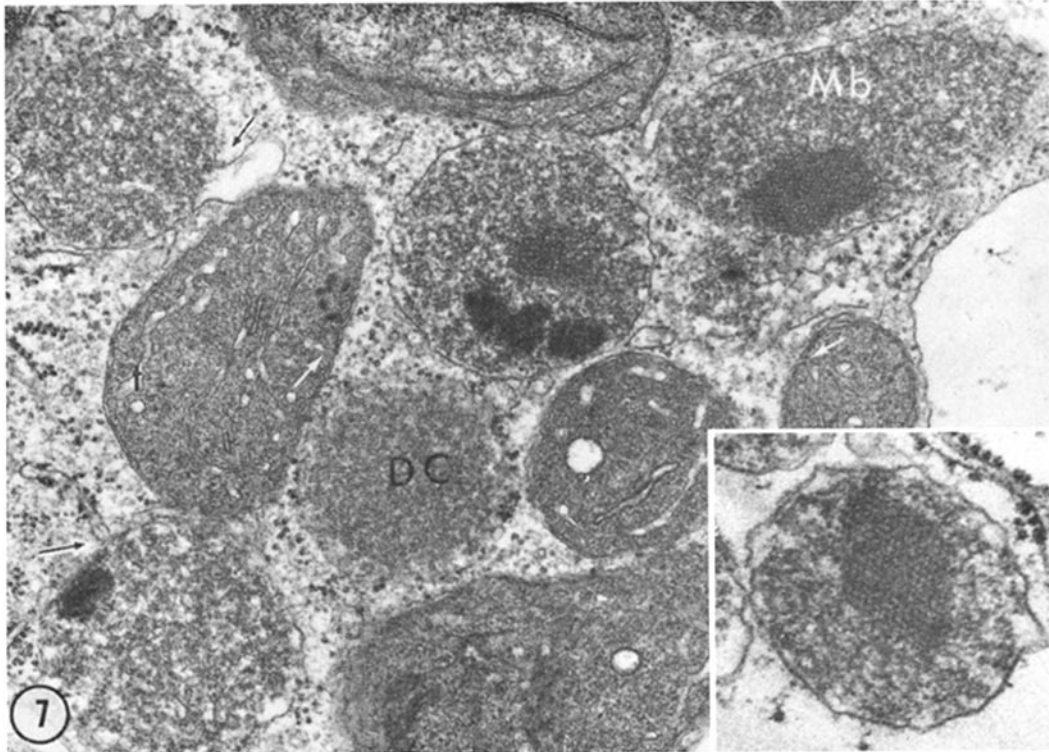
oxidized DAB consistent with microbody distribution in Zones I–III (Figs. 9–13). While there is no evidence for any soluble peroxidase in these cells, the light staining of cell walls in regions of the middle lamella facing intercellular spaces (arrows, Fig. 12) indicates that some of the tissue browning is attributable to the activity of cell wall peroxidase(s). Sections from Zone III are stained a darker brown in comparison to sections of Zones I, II, and IV because of the increased number of microbodies.

The specificity of the DAB reaction for catalase in microbodies was tested by using inhibitors. Tissue staining was not observed even after 90 min of incubation of sections in a DAB medium containing a high level (1%) of H_2O_2. Moreover, no deposition of oxidized DAB in microbodies could be detected in the electron microscope. Since vigorous oxygen release occurred during incubation, it is concluded that the catalatic action of catalase was favored by the 1% H_2O_2 concentration in the medium to the exclusion of the peroxidatic reaction involving the oxidation of DAB (23).

Addition of 0.02 M 3-amino-1,2,4-triazole (AT), a known inhibitor of catalase (39), to the complete DAB medium prevented staining of microbodies (Fig. 18) but did not prevent tissue browning due to cell wall peroxidase(s). However, potassium cyanide at a concentration of 0.1 M inhibited tissue browning as well as microbody staining.

The results of these experiments, summarized in Table II, demonstrate that oxidation of DAB in microbodies of castor bean endosperm cells is due entirely to the peroxidatic activity of catalase, and endogenous production of H_2O_2 by several microbody (glyoxysome) enzymes can sustain this reaction even when H_2O_2 is removed from the DAB medium.

While removal of H_2O_2 from the reaction medium greatly reduced tissue browning, microbodies still contained oxidized DAB (Table II). Biochem-

ical studies (16, 19) on microbodies (glyoxysomes) have demonstrated the presence of at least three enzymes that produce H_2O_2. If DAB oxidation in microbodies in the absence of H_2O_2 is the result of endogenous formation of H_2O_2 by these enzymes, addition of an inhibitor such as sodium pyruvate (1, 2) should abolish this staining (23) by reducing the endogenous H_2O_2 concentration available to glyoxysomal catalase. In order to verify the involvement of catalase in this reaction, 0.01 M potassium cyanide and 0.02 M aminotriazole were used separately and both were effective in preventing DAB oxidation in microbodies in the absence of exogenously added H_2O_2, as was also 0.002 M sodium pyruvate (Table II).

DISTRIBUTION OF OXIDIZED DAB IN MICROBODIES: Thin sections from tissue incubated in DAB showed that the electron-opaque osmium black completely filled the interior of microbodies (Figs. 9, 11, 13, and 16). The reaction product in these organelles was either finely granular and thus appeared more opaque (Figs. 9 and 16), or of a coarser nature which imparted a mottled appearance to the matrix (Figs. 11 and 13). This staining pattern, however, was very much altered in those microbodies with large crystalloids as illustrated in Fig. 17. Here the reaction product in the matrix was more diffuse and resembled a random arrangement of threadlike filaments. The only major concentration of oxidized DAB in the organelle was that over the crystalloid, where clear, unstained areas of the lattice stood out against the stained bands and accentuated the crystalline structure. Fibrous or tubular strands attached to the exposed edges of the crystalloid (arrows, Fig. 17), because they are heavily stained, can be followed in the matrix for some distance away from the crystal. It seems from these observations that catalase present initially in the matrix condenses into compact units before incorporation into the crystal and that once a crystal is formed,

FIGURE 9   Light micrograph of cells in Zone I following incubation in the complete DAB medium. The sparse, particulate distribution of reaction product shows that only a small number of microbodies (*Mb*) are present in cells of imbibed tissue. Aleurone grain (*AG*); crystalloid (*Cr*); globoid (*G*). × 1400. The electron micrograph in the *inset* illustrates the finer details of microbody staining with DAB. UA/Pb. × 30,000.

FIGURE 10   Phase micrograph of DAB-treated tissue (Zone II), showing the increase in microbodies (black particles) within these cells. Nucleolus (*Nu*); aleurone grain (*AG*). × 1400.
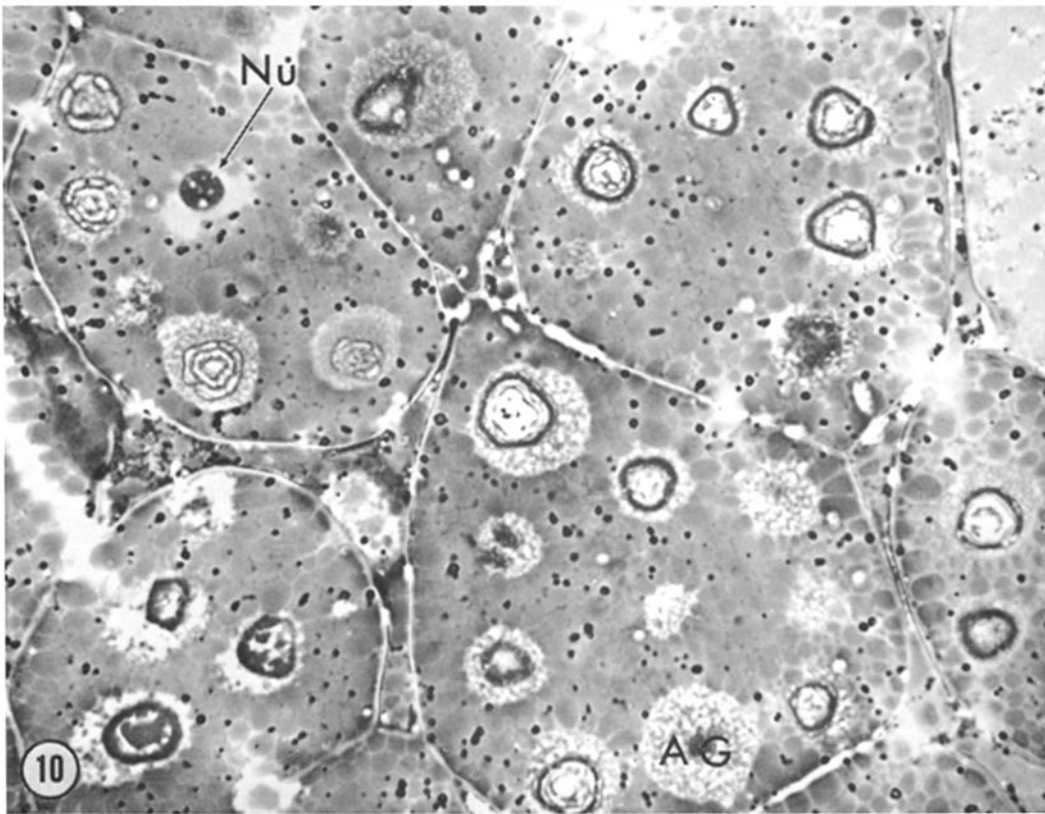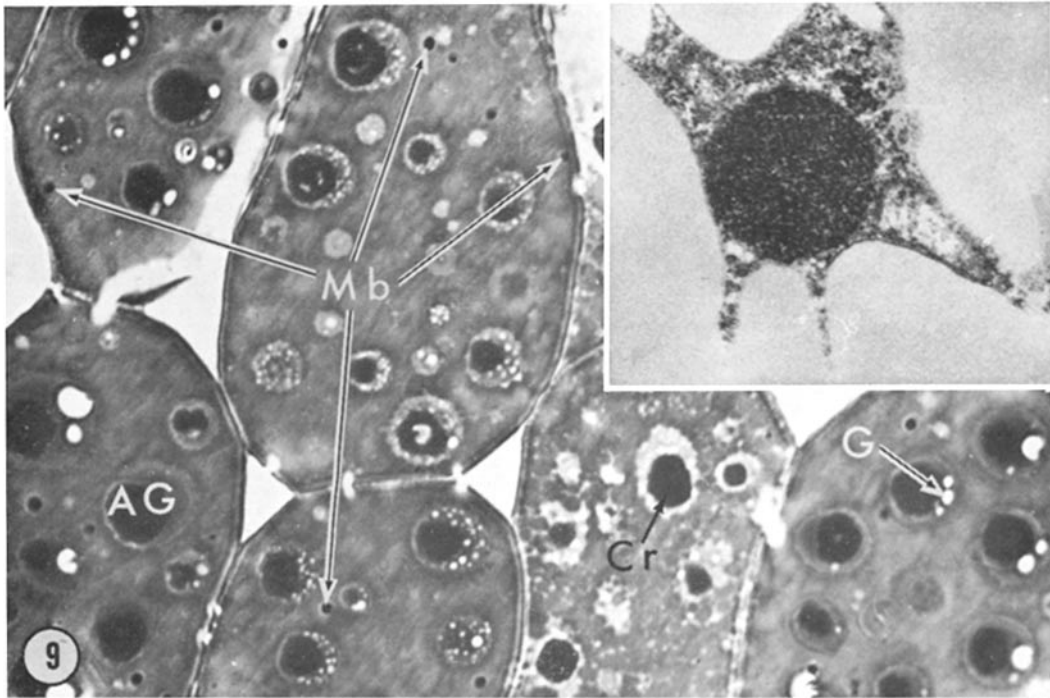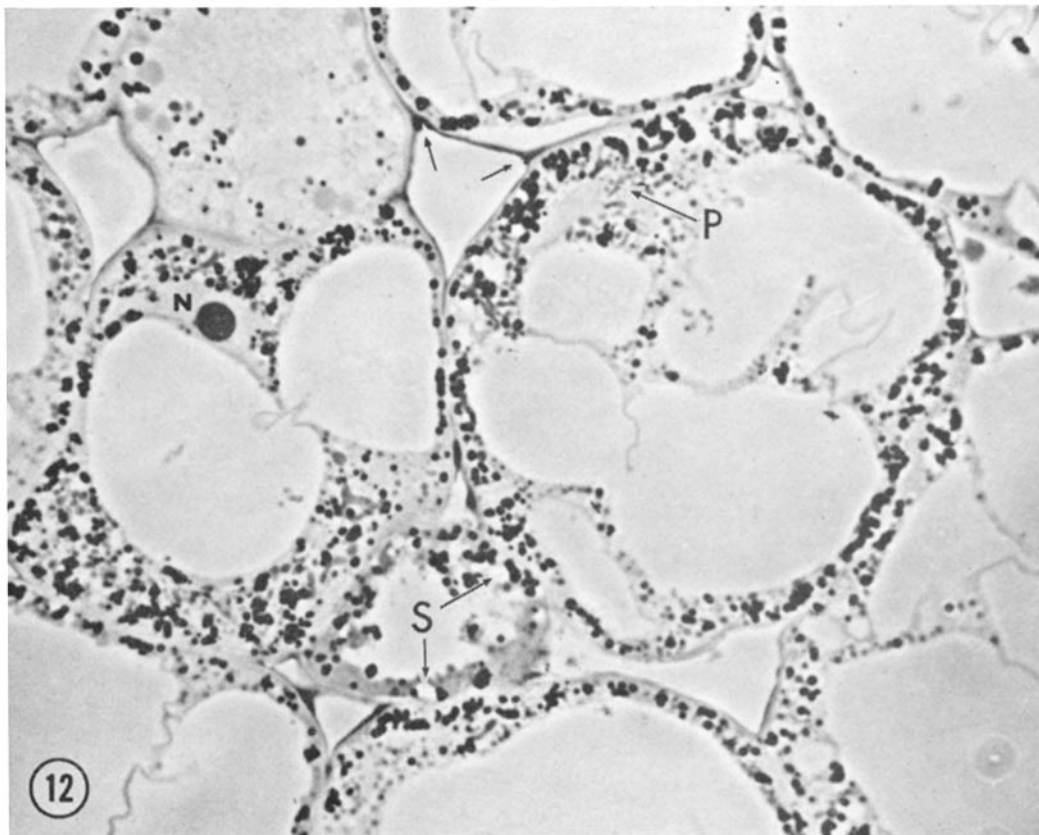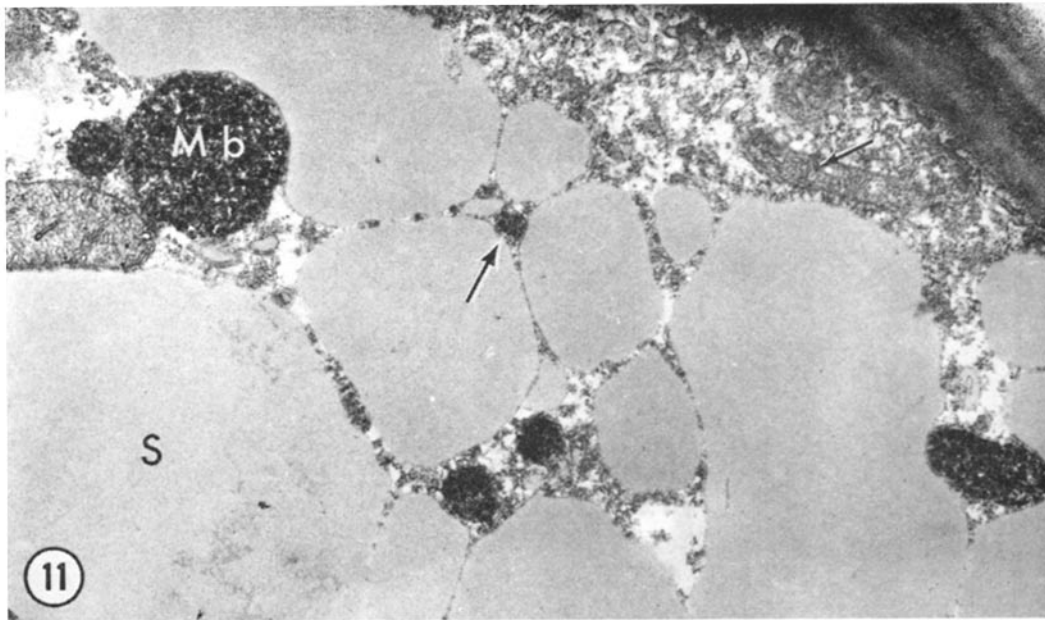
FIGURE 11 Portion of a cell from Zone II which has been stained with DAB. The microbodies (*Mb*) with their dense osmium black stand out markedly against the light background of spherosomes (*S*). Strong peroxidatic activity is evident in both small (large arrow) and large microbodies. Characteristic staining of mitochondrial cristae is also noticeable (smaller arrow). UA/Pb. × 25,000.

FIGURE 12 Light micrograph of representative cells in Zone III incubated in complete DAB medium. Note the large amount of particle-bound osmium black (microbodies) exclusively within the cytoplasm. The larger black particles are probably not enlarged microbodies but result from organelle superimposition in the section. A few spherosomes (*S*) present in these cells are surrounded by microbodies, while plastids (*P*) are not. Some DAB staining is evident along the middle lamellar regions opening into intercellular spaces (arrows). Nucleus (*N*). × 1140.
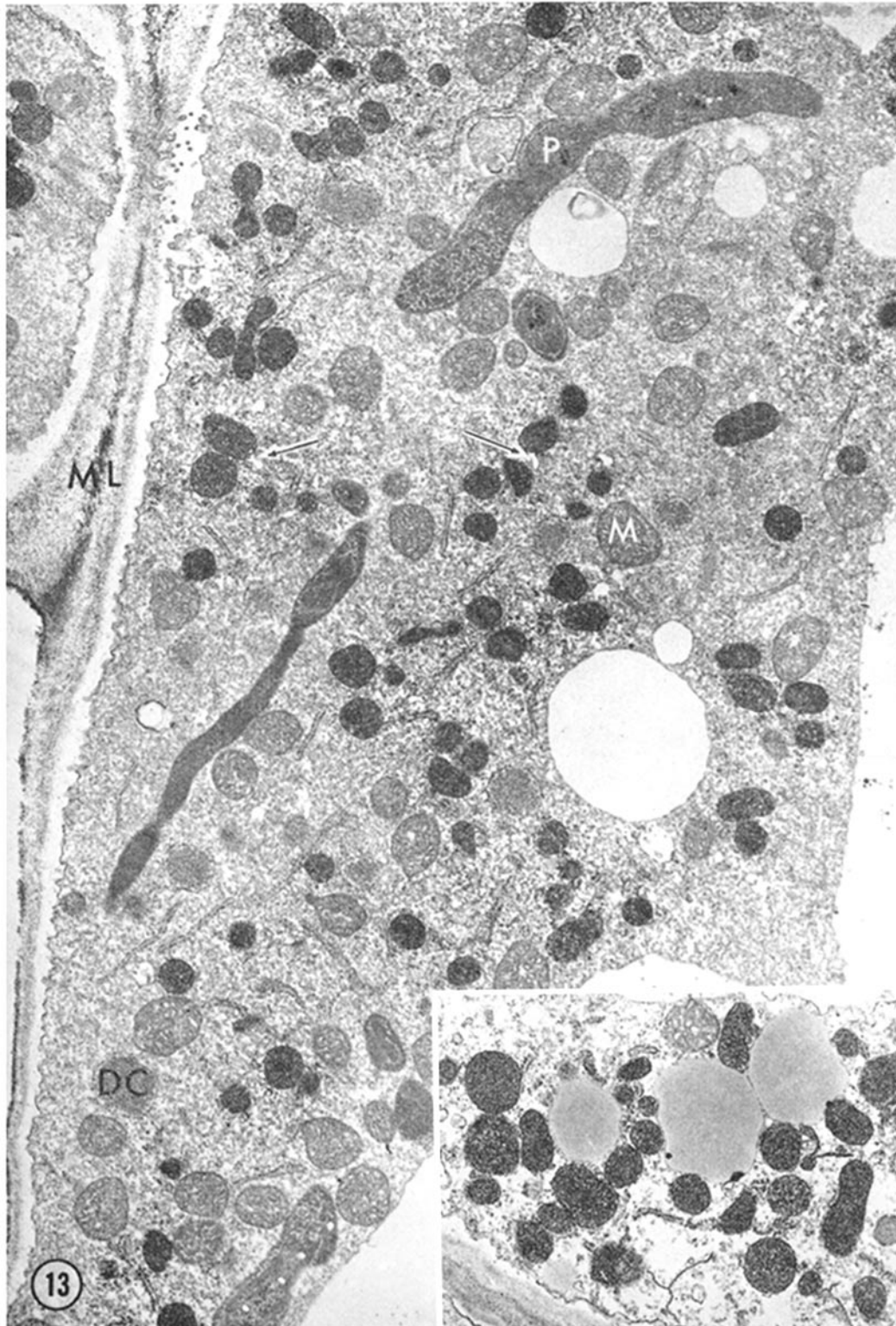
FIGURE 13 Portion of a cell from Zone III stained with DAB. The specificity of DAB staining in microbodies is clearly demonstrated by the absence of reaction product in plastids (*P*), dilated cisternae (*DC*), and ground cytoplasm. There is, however, light staining of cristae in mitochondria (*M*) and in the middle lamella (*ML*). Tails on microbodies (arrows) do not contain oxidized DAB. Section not contrasted with heavy metals. × 12,300. The spherosomes in the *inset* are surrounded by microbodies densely stained with DAB. UA/Pb. × 8340.
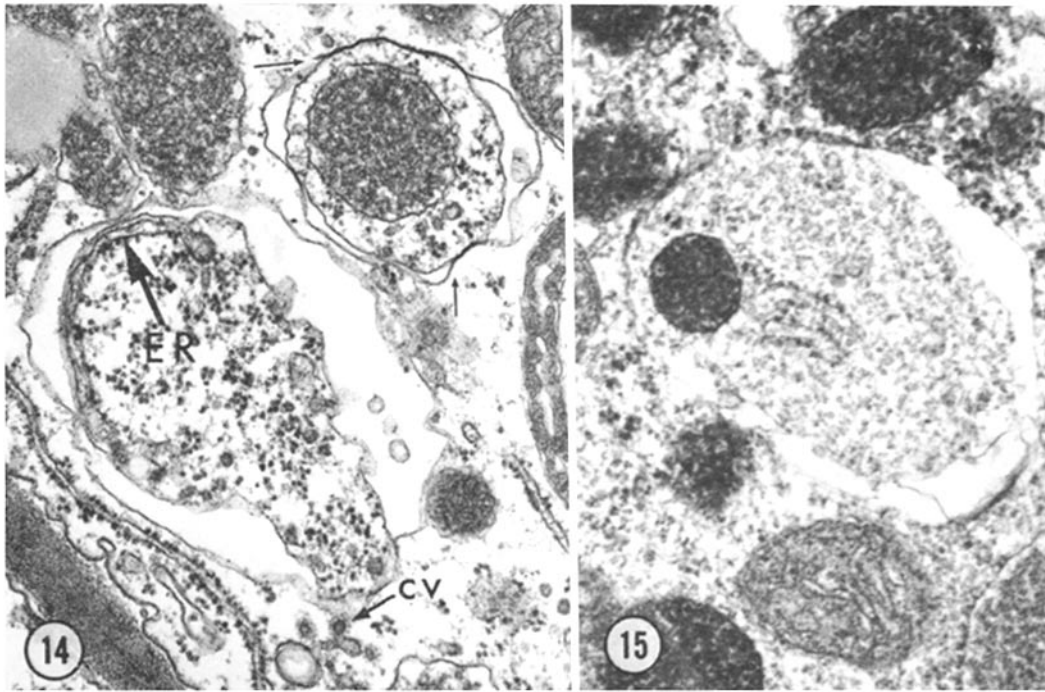
FIGURE 14   Segregation of cytoplasmic material by double-membraned cisternae. The limiting membranes of the larger vacuole with a segment of rough *ER* and many free ribosomes appear separate, while those of the smaller vacuole containing a microbody and a few ribosomes are partially fused (arrows). Several coated vesicles (*cv*) are near an unfused limiting membrane. Tissue stained with uranyl acetate. Section contrasted with lead citrate. × 35,000.

FIGURE 15   Sequestered microbody in an autophagic vacuole from tissue incubated in the complete DAB medium. Note the uniformity in density of osmium black over the matrix of the sequestered microbody and of those microbodies free in the cytoplasm. UA/Pb. × 28,000.

TABLE II

Inhibition of DAB Staining in Microbodies of Castor Bean Endosperm

	Control	1% H₂O₂	0.1 M KCN	0.01 M KCN	0.02 M AT	0.002 M Pyruvate
Complete medium	++	—	—		—	
Without H₂O₂	+			—	—	—

soluble catalase is restricted to the matrix around the crystal. Examination of crystal-containing microbodies from tissue segments exposed to the catalase inhibitor aminotriazole presented a striking contrast to the DAB-stained microbodies by the absence of any visible reaction product in both the matrix and over the crystalloid (Fig. 18). The

absence of DAB in the interstices of the crystalloid serves to distinguish catalase distribution in plant microbodies from that in rat liver microbodies where the finely granular reaction product is uniformly distributed throughout the matrix, even permeating the lumen of the nucleoid, but never occurring on the tubules (23).

DISCUSSION

Fine structural and cytochemical changes related to biochemical and physiological events occurring during germination were observed in the four zones in castor bean endosperm. Most obvious are disappearance of stored food reserves and vacuolation of the cells. Microbodies (glyoxysomes) are present in all cells from inhibition to cellular lysis and show a striking increase in size and number. Parallel but less dramatic changes also occur in mitochondria, plastids, and other cellular structures. These

events require synthesis of proteins and, therefore, are contingent on the assembly of the protein synthetic apparatus that is almost nonexistent in the dry seed (see review, 40). Some of the enzymes involved in the metabolism of food reserves, however, have been shown to be activated by hydration (10, 17, 18, 50) while others are synthesized *de novo* (3, 4, 41). In this regard endosperm of castor bean differs from storage tissue in other seeds by the conspicuous low level of cytoplasmic ribosomes and ER in dry and hydrated tissue (5, 14, 57, 58) as a result of ribosome degradation during seed ripening (58). Monosomes appear within 24 hr of hydration in castor bean endosperm, and complete reassembly of the ribosomal apparatus is evident at 72 hr when polysomes are the site of maximum radioactivity from ^{32}P incorporation into RNA (41).

Microbodies

Cell particulates have been isolated from homogenates of leaf and endosperm which contain enzymes involved in photorespiration and the formation of succinate from fatty acids. These have been termed peroxisomes and glyoxysomes, respectively (61, 13). Morphologically, however, they are very similar, and should be considered as specializations of the class of microbodies. Since fine structural studies demontrate that microbodies are a virtually constant feature of plant cells (26, 47), one can expect that other biochemical studies may well indicate yet other specializations of enzyme composition that depend on the ever present catalase (67) to metabolize endogenous H_2O_2. The participation of microbodies in endosperm cells in reactions other than gluconeogenesis is suggested by the presence of urate oxidase and allantoinase in isolated glyoxysomes (19). The universal distribution of plant microbodies and their enzymatic heterogeneity can be contrasted with the more limited distribution and function of microbodies in kidney and liver cells of animals, as well as in protozoa (19, 35).
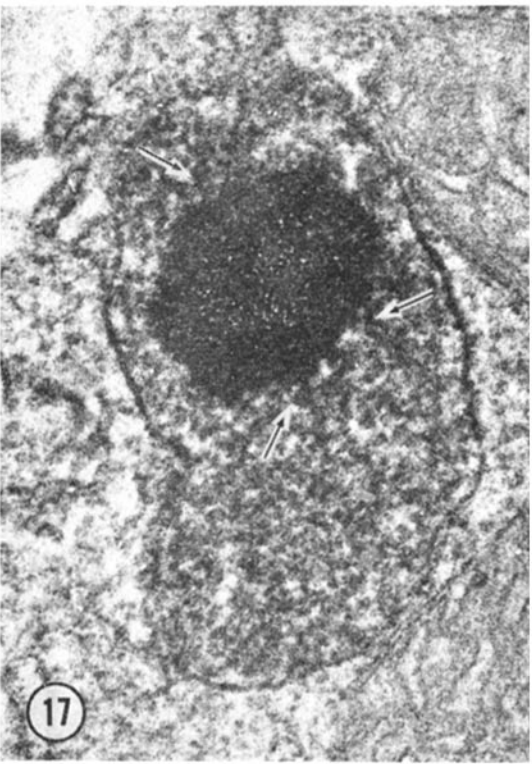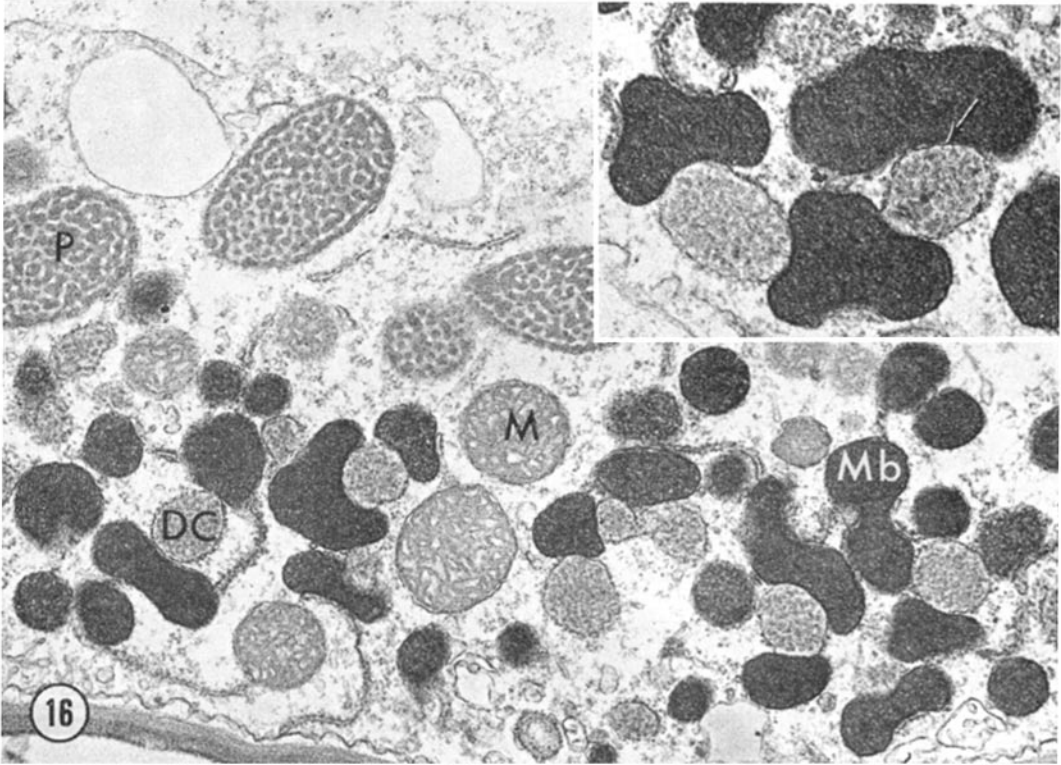
The observations of McGregor and Beevers (44) have a direct bearing on the problem of terminology and function for microbodies. When they followed the time course of malate synthetase and isocitrate lyase activity in isolated glyoxysomes from cotyledons of germinating watermelon seeds, they found an initial increase and a later decrease, similar to that in castor bean endosperm (30), that paralleled the depletion of stored lipid. Exposure

of cotyledons to light after 4 days of growth in the dark resulted in complete disappearance of the glyoxysomal enzymes malate synthetase and isocitrate lyase over the next 4 days. However, during this period there was a striking increase in enzymes associated with photosynthesis, two of which (glycolate oxidase and glyoxylate reductase) were bound to particles sedimenting at the same density of glyoxysomes, being that of peroxisomes from leaf cells (19). Although the cytological events associated with these changes are presently unclear, it seems likely that either the microbody population is able to change its enzyme composition or that exposure to light has stimulated the formation of a new microbody population.

Because of the enzymatic heterogeneity demonstrated in plant microbodies of various kinds, care must obviously be exercised in utilizing specific marker systems in biochemical studies. For example, the use of isocitrate lyase and malate synthetase as marker enzymes for glyoxylate cycle activity in particles from various plant tissues by Cooper and Beevers (15), while demonstrating the presence or absence of glyoxysomes, overlooks the possible occurrence of microbodies lacking these glyoxylate cycle enzymes. In addition, certain microbodies have been shown to be particularly sensitive to osmotic changes (30, 61, and unpublished data) and thus can easily be lost during homogenization and purification. The combined analysis of tissues by both electron microscopy and biochemical methods thus seems desirable.

DEVELOPMENT AND TURNOVER: A direct attachment between the microbody membrane and rough or smooth ER has been reported in livers of fetal and adult rats and mice (20, 21, 46, 63). This has suggested to several investigators that microbodies may be formed directly from ER by a process of budding, rather than through an accumulation in membranes of the Golgi apparatus as established for secretion granule formation. As illustrated in the present study, plant microbodies also show membrane continuity with rough ER, suggesting a mode of formation similar to that in animal cells.

The increased abundance of microbodies in castor bean endosperm parallels the increase in isocitrate lyase and malate synthetase activity in glyoxysomes during the first 5 days of germination as described by Gerhardt and Beevers (30). Following the linear rise in enzyme activity, there is a decline after day 5 which parallels a similar reduction in glyoxysome proteins. Our studies of endo-

sperm cells at a comparable age showed that at least some microbodies disappear *in toto* by sequestration into autophagic vacuoles. By cytochemical examination, sequestered microbodies contain a very active catalase (Fig. 15), indicating that loss in enzyme activity does not occur prior to digestion. Glyoxysome turnover, therefore, must result in the loss of a whole group of enzymes as one single event. It thus appears that the decrease in total protein and specific activity of isocitrate lyase and malate synthetase in the glyoxysome band, as reported by Gerhardt and Beevers (30), resulted at least in part from the sequestration and subsequent destruction of microbodies in digestive vacuoles.

Incorporation of leucine-^{14}C into glyoxysomal protein at day 5 (30) also suggested that a continuous turnover occurs in microbody proteins. In light of the present observations, this protein turnover could be interpreted in several ways. First, the large variation in the diameters of microbodies and their increased number in Zone III indicates that new organelles are continually formed. Second, the continuity of microbody membranes with a segment of rough ER may also represent a means whereby new proteins are continuously supplied to the organelle, although such connections are most frequently observed in smaller, and probably forming, microbodies. There is a third possibility that mature microbodies can incorporate proteins made elsewhere, in a manner similar to that whereby mitochondria of mammalian tissues incorporate certain respiratory enzymes

made in the cytoplasm (59). Lastly, it is likely that dilated cisternae were present as a contaminant in glyoxysome bands within the gradient and much of the observed incorporation might be attributable to these components.

SPECIFICITY OF THE DAB REACTION: The ability of heme proteins to oxidize DAB and the finely disperse nature of its polymerized end product (54) make this compound ideally suited for studying the intracellular distribution of heme enzymes involved in peroxidatic and redox reactions in plant and animal cells. In addition endogenous (8, 23, 25, 64–67) and injected (22) catalase, other heme proteins that have been studied include endogenous (7, 9, 66, 67) and injected (28, 29, 33) peroxidase and cytochromes (8, 54, 66, 67).

The staining pattern of endosperm tissue incubated in DAB demonstrates cell wall peroxidase(s) and catalase in microbodies. The presence of catalase in microbodies was confirmed by the use of aminotriazole, potassium cyanide, and a high H_2O_2 concentration in DAB media. Microbody staining still occurred when H_2O_2 was removed from the medium, but this could also be eliminated by treatment with sodium pyruvate or addition of either aminotriazole or potassium cyanide. This indicates that endogenous generation of H_2O_2 as a catalase substrate could still occur following fixation of the tissue in glutaraldehyde. The presence of three known enzymes in glyoxysomes which produce H_2O_2, i.e. glycolic oxidase (13), an oxygen requiring (FAD-linked) fatty acyl-CoA dehydro-

FIGURE 16 Portion of a DAB-stained cell (Zone III), with numerous microbodies (*Mb*) and dilated cisternae (*DC*) closely appressed. The dense reaction product, being only in the microbodies, accentuates this spatial association which may involve more than one organelle but not mitochondria (*M*) and plastids (*P*). UA/Pb. × 12,300. The arrow in the *inset* points to the region of apposition between a microbody and dilated cisterna membrane where the absence of membrane-bound ribosomes allows for a closer association to the microbody. UA/Pb. × 19,900.

FIGURE 17 High resolution micrograph of a crystal-containing microbody stained with DAB. The weakly stained matrix contrasts with the very dense staining over the crystalloid. The small clear spaces within the crystalloid indicate that only the tubules or dense bands of the core are the site of activity. Along the periphery of the crystal, stained tubular or fibrillar units (arrows) that are continuous with the crystal lattice extend for some distance in the surrounding matrix. UA/Pb. × 68,600.

FIGURE 18 Appearance of a microbody following incubation with 0.02 M amino-triazole in the complete DAB medium. The absence of any reaction product in the matrix or crystalloid clearly demonstrates the enzymatic nature of the staining reaction, in addition to providing a striking comparative image with respect to Fig. 17. UA/Pb. × 48,000.

genase (16), and urate oxidase (19), was apparently responsible for DAB oxidation by catalase in microbodies following incubation in DAB minus H_2O_2.

CRYSTALLOID STAINING WITH DAB: The specific localization of catalase in the crystalloid of endosperm microbodies parallels the pattern of catalase localization in the crystalloid of microbodies in oat coleoptile cells (64) and elsewhere (25, 66, 67). Structural differences involving the size and spacing of lattice components, however, exist between coleoptile and endosperm crystalloids, suggesting that different plant microbody cyrstalloids may involve different proteins or be complexes of several proteins. The electron-opaque units of coleoptile crystalloids are approximately 60 by 85 A in size, with lattice spacings averaging 130 and 110 A, respectively (unpublished data). In endosperm microbodies shown here, crystalloids have a uniform dimension of about 60 A and, thus, a constant lattice spacing of 110 A. Even though crystalloids in microbodies of different tissues differ in size and substructure, the DAB reaction invariably demonstrates that they are still the principal site of catalase within the cell (66, 67).

Dilated Cisternae

Dilated cisternae presumably represent an organelle not directly related to microbodies or their development, since they form only in cells of Zone III, at a time when microbodies are already maximally abundant. Also, their dense matrix material is unreactive to DAB oxidation. As mentioned above, it is possible that they may be a contaminant in preparations of glyoxysomes obtained by density gradient centrifugation. If so, the fact that they are surrounded by a ribosome-bearing membrane might account for the report (31) of the presence of microbody RNA. The closeness of microbodies to dilated cisternae (Fig. 16) suggests that the latter may be a source of metabolites for microbodies as are spherosomes.

Aleurone Grains

Aleurone grains are the major source of reserve protein in seeds. These proteins have high concentrations or arginine, asparagine, and glutamine (6). Besides proteins, aleurone grains also contain insoluble salts of phytic acid (32, 62) and crystals of calcium oxalate (6). Detection of several hydrolytic enzymes in aleurone grains by biochemical analysis of isolated grains (42, 68) or by ultra-

structural cytochemistry (52) have suggested to these workers that aleurone grains are similar to the lysosomes of animal cells. It would seem logical to limit the concept of lysosome, however, to include bodies formed through phagocytic or autophagic processes. The aleurone grains are probably more closely analogous to yolk platelets of vertebrate embryos as membrane-bounded organelles containing reserves of proteins. Like aleurone grains in germinating seeds, the yolk platelets of embryos also become rich in hydrolytic enzymes which facilitate the release of breakdown products to the cell (36a).

Spherosomes

Earler studies on the fine structure and development of spherosomes or lipid bodies in plant cells (27, 34) relied heavily on potassium permanganate fixation and did not distinguish between the various membrane systems and vacuole formation (45) in the cell. The relation between spherosomes and other membrane-bounded organelles was therefore unclear. The suggestion that spherosomes arise from endoplasmic reticulum as protein vacuoles, transform into lipid bodies, and subsequently into lysosomes has not been generally accepted (56). Our observations show that spherosomes do not convert to autophagic vacuoles but instead decrease in size and ultimately disappear from endosperm cells during seed germination.

The function of spherosomes in storage tissues has not been completely elucidated, although Matile and Spichiger (43) have suggested that they are similar to lysosomes of animal cells because they contain similar hydrolytic enzymes. Included among the hydrolases that they studied were RNase and DNase. However, electron micrographs of isolated particles were not presented, leaving open the possibility that their preparations were contaminated with other organelles. Fine structural evidence presented here shows that spherosomes are often closely associated with other organelles and rough ER. The presence of lipase in isolated spherosomes (51) suggests that their main function in castor bean endosperm tissue is, like aleurone grains, one of storage and subsequent utilization during germination to provide fatty acids for microbodies which can readily convert the acyl-CoA derivatives to succinate (16). The large amount of triglycerides in isolated lipid bodies from shoot apices of young corn seedlings

(62a) is a further indication of the storage role for lipid bodies (spherosomes) in plant cells.

Mitochondria and Plastids

The important role of mitochondria during germination is apparent by their twofold increase in number and extensive crista formation between Zones II and III. It is clear from a combined biochemical and fine structural study of mitochondria from endosperm of germinating castor beans (5) that the increase in cristae directly relates to the presence of respiratory enzymes in the isolated mitochondria. In addition, Akazawa and Beevers (3) have shown an increase in activity of respiratory enzymes and ATP formation in mitochondria of castor bean endosperm during germination. NADH is a product of succinate formation in glyoxysomes (16); but glyoxysomes, like the peroxisomes of animal cells (19), lack the electron transfer enzymes of mitochondria to oxidize reduced nucleotides to form ATP. It is thus apparent that ATP generation could well involve the interaction of both organelles, as is true for malate formation (15).

Mitochondria isolated from castor bean do not metabolize succinate through the TCA cycle but transform this glyoxysome end product into oxaloacetate (15). Oxaloacetate is subsequently converted to sucrose by the action of several soluble enzymes in the cytoplasm (15) and enzymes in plastids (38). Fine structural changes in plastids observed in the present study document the development of proplastids to leucoplasts that contain an elaborate tubular complex, occupying a considerable volume in the organelle. These tubules develop as invaginations of the inner membrane of the plastid envelope and subsequently anastomose into a netlike array, representing the major developmental change during their threefold increase in number between Zones II and III. Tubules in plastids of permanganate-fixed endosperm tissue have been reported previously (49), but the intricate network illustrated here was not observed. It appears likely that enzymes involved in gluconeogenesis are associated with these tubules.

The fine structural and cytochemical changes observed in endosperm of germinating castor beans complement earlier biochemical studies which indicated that several organelles, viz. microbodies, mitochondria, and plastids, coordinated their functions in the conversion of stored food reserves into smaller molecular weight compounds. These compounds, sucrose and amino acids predominating, are readily transported to the developing seedling. Physical and biochemical interaction between various organelles in the endosperm thus play an important role during the transition period in the young seedling from heterotrophy to autotrophy.

REFERENCES

1. Aebi, H., J. Quitt, and A. Hasson. 1962. *Helv. Physiol. Pharmacol. Acta.* 20:148.
2. Aebi, H., F. Stocker, and M. Eberhardt. 1963. *Biochem. Z.* 336:526.
3. Akazawa, T., and H. Beevers. 1957. *Biochem. J.* 67:115.
4. Alberghina, F. 1964. *G. Bot. Ital.* 71:385.
5. Albergoni, F., P. Lado, G. Marziani, and E. Marrè. 1964. *G. Bot. Ital.* 71:469.
6. Altschul, A. M., L. Y. Yatsu, R. L. Ory, and E. M. Engleman. 1966. *Annu. Rev. Plant Physiol.* 17:113.
7. Bainton, D. F., and M. G. Farquar. 1968. *J. Cell Biol.* 39:299.
8. Beard, M. E., and A. B. Novikoff. 1969. *J. Cell Biol.* 42:501.
9. Behnke, O. 1969. *J. Histochem. Cytochem.* 17:62.
10. Bianchetti, R., and M. P. Cornaggia. 1965. *G. Bot. Ital.* 72:370.
11. Bonnett, H. T., Jr., and E. H. Newcomb. 1965. *J. Cell Biol.* 27:423.

12. BREIDENBACH, R. W., and H. BEEVERS. 1967. *Biochem. Biophys. Res. Commun.* 27:462.
13. BREIDENBACH, R. W., A. KAHN, and H. BEEVERS. 1968. *Plant Physiol.* 43:705.
14. COCUCCI, S., R. MAGGIO, A MONROY, and E. MARRÈ, 1965. *Rend. Accad. Nazl. Lincei.* 38:545.
15. COOPER, T. G., and H. BEEVERS. 1969. *J. Biol. Chem.* 244:3507.
16. COOPER, T. G., and H. BEEVERS. 1969. *J. Biol. Chem.* 244:3514.
17. CORNAGGIA, M. P. 1964. *G. Bot. Ital.* 71:503.
18. CORNAGGIA, M. P., and E. MARRÈ. 1964. *G. Bot. Ital.* 71:515.
19. DE DUVE, C., and J. T. HOGG. The Nature and Function of Peroxisomes (Microbodies, Glyoxysomes). Conference held by the New York Academy of Science. May, 1969.
20. ESSNER, E. 1967. *Lab. Invest.* 17:71.
21. ESSNER, E. 1969. *J. Histochem. Cytochem.* 17:454.
22. VENKATACHALAM, M. A., and H. D. FAHIMI. 1969. *J. Cell Biol.* 42:480.
23. FAHIMI, H. D. 1969. *J. Cell Biol.* 43:275.
24. FREDERICK, S. E., and E. H. NEWCOMB. 1969. *Science (Washington).* 163:1353.
25. FREDERICK, S. E., and E. H. NEWCOMB. 1969. *J. Cell Biol.* 43:343.
26. FREDERICK, S. E., E. H. NEWCOMB, E. L. VIGIL, and W. P. WERGIN. 1968. *Planta.* 81:229.
27. FREY-WYSSLING, A., E. GRIESHABER, and K. MÜHLETHALER. 1963. *J. Ultrastruct. Res.* 8:506.
28. FRIEND, D. S. 1969. *J. Cell Biol.* 41:269.
29. FRIEND, D. S., and M. G. FARQUAR. 1967. *J. Cell Biol.* 35:357.
30. GERHARDT, B. P., and H. BEEVERS. 1970. *J. Cell Biol.* 44:94.
31. GERHARDT, B. P., and H. BEEVERS. 1969. *Plant Physiol.* 44:1475.
32. GIBBINS, L. N., and F. W. NORRIS. 1967. *Biochem. J.* 86:64.
33. GRAHAM, R. C., JR., and M. J. KARNOVSKY. 1966. *J. Histochem. Cytochem.* 14:291.
34. GRIESHABER, E. 1964. *Vjschr. Naturforsch. Ges. Zurich.* 109:1.
35. HRUBAN, Z., and M. RECHCIGL, JR. 1969. *Int. Rev. Cytol.* 1(Suppl.):1.
36. JACKS, T. J., L. Y. YATSU, and A. M. ALTSCHUL. 1967. *Plant Physiol.* 42:585.
36a. KARASAKI, S. 1963. *J. Ultrastruct Res.* 9:225.
37. KEILIN, D., and E. F. HARTREE. 1936. *Proc. Roy. Soc. (London), Ser. B.* 119:141.
38. KOBR, M. J., and H. BEEVERS. 1968. *Plant Physiol.* 43:S-17.
39. MARGOLIASH, E., and A. NOVOGRODSKY. 1958. *Biochem. J.* 68:468.
40. MARRÈ, E. 1967. Current Topics in Developmental Biology. A. Monroy and A. A. Moscona, editors. 2:75.
41. MARRÈ, E., S. COCUCCI, and S. STURANI. 1965. *Plant Physiol.* 40:1162.
42. MATILE, PH., 1968. *Z. Pflanzenphysiol.* 58:365.
43. MATILE, PH., and J. SPICHIGER, 1968. *Z. Pflanzenphysiol.* 58:277.
44. McGREGOR, D. I., and H. BEEVERS, 1969. *Plant Physiol.* 44:S-33.
45. MESQUITA, J. F. 1969. *J. Ultrastruct. Res.* 26:242.
46. MOCHIZUKI, Y. 1968. *Tumor Res.* 3:1.
47. MOLLENHAUER, H. H., D. J. MORRÈ, and A. G. KELLY. 1968. *Protoplasma.* 62:44.
48. NOVIKOFF, A. B., and S. GOLDFISCHER. 1968. *J. Histochem. Cytochem.* 16:507.
49. ORSENIGO, M., 1964. *G. Bot. Ital.* 71:43.
50. ORY, R. L., A. J. ST. ANGELO, and A. M. ALTSCHUL. 1962. *J. Lipid Res.* 3:99.
51. ORY, R. L., L. Y. YATSU, and H. W. KIRCHER. 1968. *Arch. Biochem. Biophys.* 123:255.
52. POUX, N. 1965. *J. Microsc.* 4:771.
53. REYNOLDS, E. S. 1963. *J. Cell Biol.* 17:208.
54. SELIGMAN, A. M., M. J. KARNOVSKY, H. L. WASSERKRUG, and J. S. HANKER. 1968. *J. Cell Biol.* 38:1.
55. SELIGMAN, A. M., R. E. PLAPINGER, and H. L. WASSERKRUG. 1969. *J. Histochem. Cytochem.* 17:192.
56. SOROKIN, H. P. 1967. *Amer. J. Bot.* 51:1008.
57. STURANI, E. 1968. *Life Sci.* 7:527.
58. STURANI, E., and S. COCUCCI. 1965. *Life Sci.* 4:1937.
59. SWICK, R. W., A. K. REXROTH, and J. L. STANGE. 1968. *J. Biol. Chem.* 243:3581.
60. SWIFT, H. and Z. HRUBAN. 1964. *Fed. Proc.* 23:1026.
61. TOLBERT, N. E., A. OESER, T. KISAKI, R. H. HAGEMAN, and R. K. YAMAZAKI. 1968. *J. Biol. Chem.* 243:5179.
62. TOMBS, M. P. 1967. *Plant Physiol.* 42:797.
62a. TRELEASE, R. N. 1969. *J. Cell Biol.* 43:147a.
63. TSUKADA, H., Y. MOCHIZUKI, and T. KONISHI. 1968. *J. Cell Biol.* 37:231.
64. VIGIL, E. L. 1969. *J. Histochem Cytochem.* 17:425.
65. VIGIL, E. L. 1969. *Plant Physiol.* 44:S-4.
66. VIGIL, E. L. 1969. *XI Intern. Botan. Congr.* 229. (Abstr.)
67. VIGIL, E. L. 1969. *J. Cell Biol.* 43:152a.
68. YATSU, L. Y., and T. J. JACKS. 1968. *Arch. Biochem. Biophys.* 124:466.